BIP-Predictor

Marc Wildi

Zurich University of Applied Sciences (ZHAW)

8000 Zurich, Switzerland

marc.wildi@zhaw.ch

May 6, 2025

Abstract

1 Introduction

2 Data and Dependence

2.1 Data

- Choice of indicators: BIP, ip, ESI, ifo, spread

- Quarterly frequency (emphasize $h \geq 2$)

- Data transformations: Diff-log, standardization (merely for ease of visual inspection), trim Covid ourliers

- Revisions and publication lags: BIP lagged by quarter and ip lagged by two months in Jan-2025 data set

- Real-time data: all series are artificially aligned at end point. BIP and ip are advanced by their lags.

The transformed quarterly series are displayed in Fig. 1, while Fig. 2 offers a close-up view of the financial crisis and the pandemic. The latter figure illustrates that the real-time GDP and industrial production series are synchronized at dips and peaks (coincident), whereas the other indicators tend to lead in relative terms. This characteristic of the additional explanatory variables can be leveraged in a multivariate approach to enhance forecasting performance compared to univariate benchmarks.

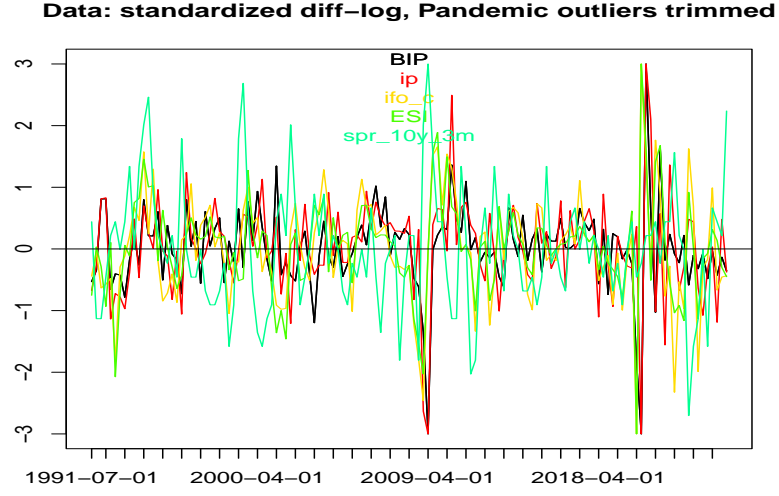**Data: standardized diff−log, Pandemic outliers trimmed**

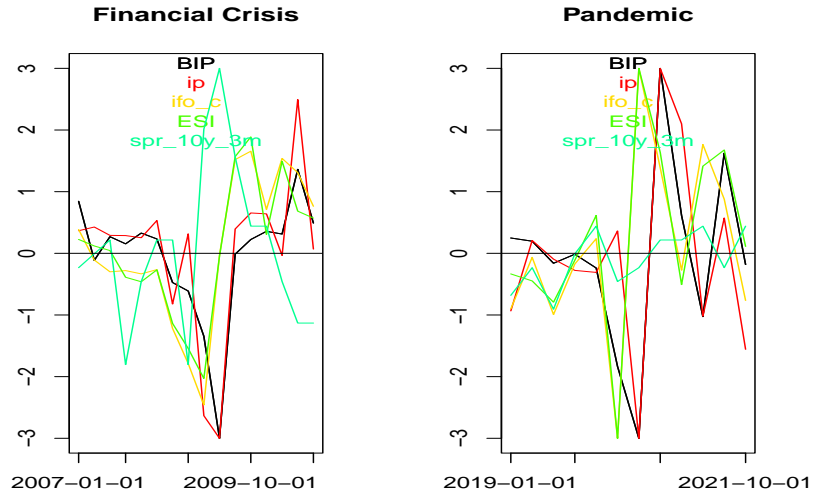Figure 1: Sample cross-correlation function (CCF): full data set.

Figure 2: Data: leads and lags during financial crisis (left) and Pandemic (right).

2.2 Dependence

We analyze the dependence structure of the data and derive a simple VAR model to establish the multivariate filter. The sample cross-correlation function (CCF) is shown in Figs. 3 (entire dataset) and 4 (data prior to the pandemic).
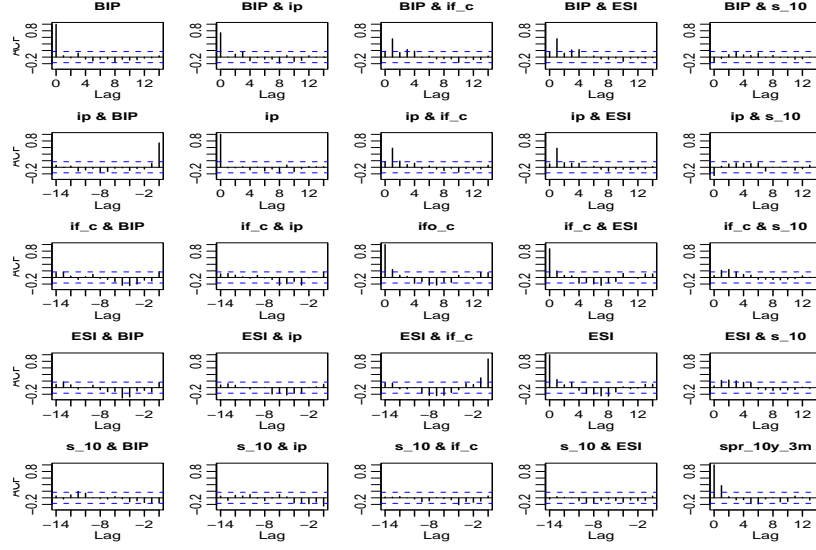
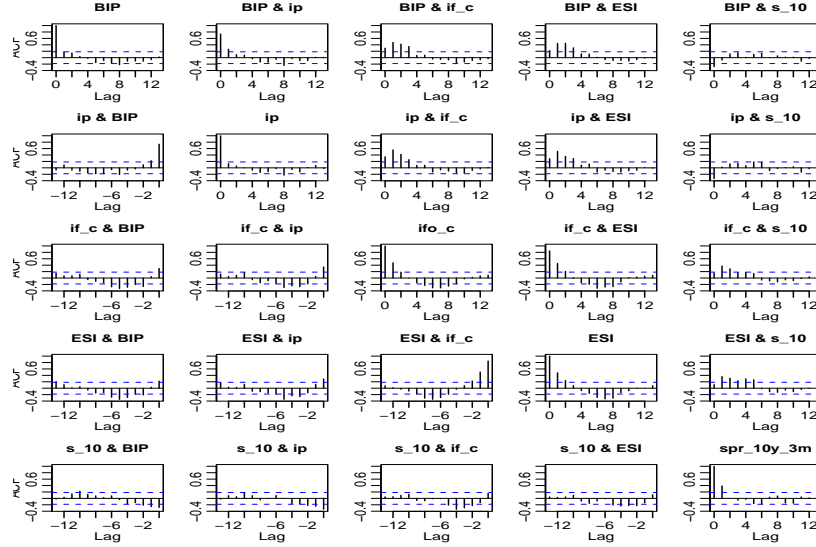Figure 3: Sample cross-correlation function (CCF): full data set.

Figure 4: Sample cross-correlation function (CCF): without Pandemic.

The CCF confirms the leads and lags illustrated in Fig. 2, although the strength of the dependence is influenced by the singular readings during the pandemic[1]. We can now fit a VARMA model, and according to standard diagnostic tests (not shown here), a simple VAR(1) specification aligns with the data. The resulting impulse responses of the model are presented in Figs. 5 (full data set) and (6) (prior the pandemic).

---

[1] We discard the corresponding data when finalizing the predictor.
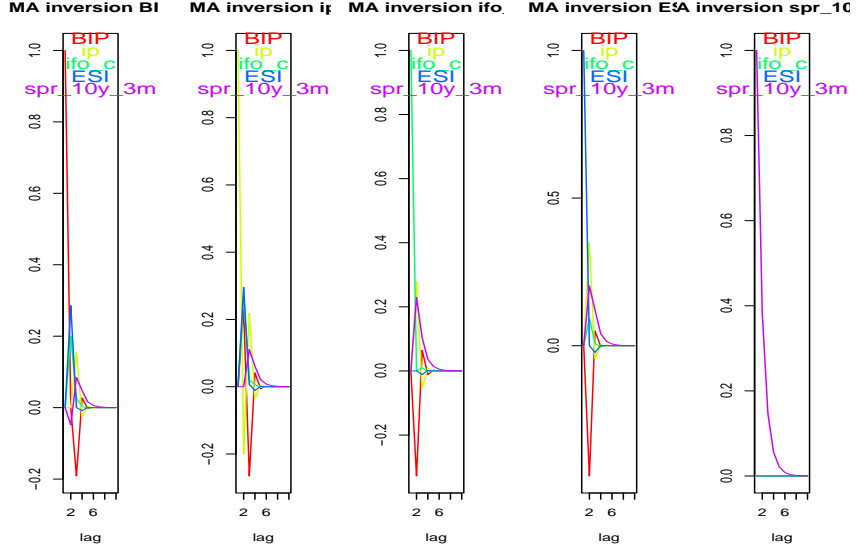
Figure 5: MA inversion of VAR(1): full data set.

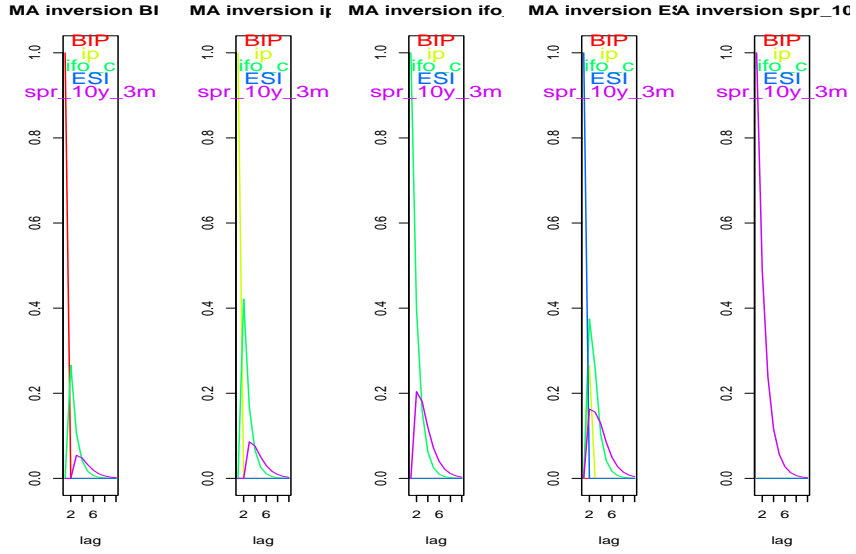Figure 6: MA inversion of VAR(1): without Pandemic.

The model summarizes key features of the data, where lagging series (GDP and industrial production, when accounting for publication lags) depend on indicators leading in relative terms. In particular, the impulse response of the spread (rightmost panel in the figure) suggests the relevance of a univariate model for this specific leading indicator.

3 Direct Forecasts

3.1 'Classic' Direct Forecast

So-called direct forecasts are obtained by regressing the relevant indicators on forward-shifted BIP, accounting for the additional publication lag. For illustration of the concept, we here rely on all indicators and full sample information, excluding the pandemic. In-sample forecasts and the shifted BIP, which serves as the target, are presented in Figs. 7 (full dataset without the pandemic) and 8 (financial crisis) for horizons up to three quarters ahead.
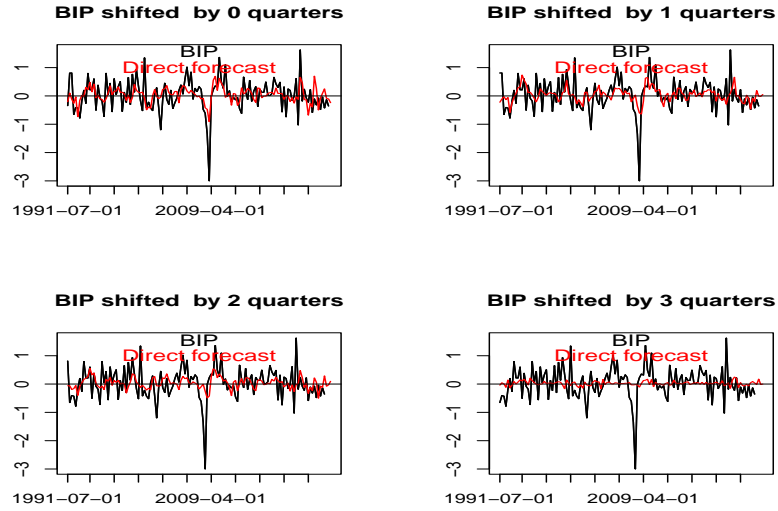

Figure 7: Direct forecasts (red lines) based on all indicators and full sample information, without the pandemic: BIP (black line) shifted by zero one, two and three quarters.
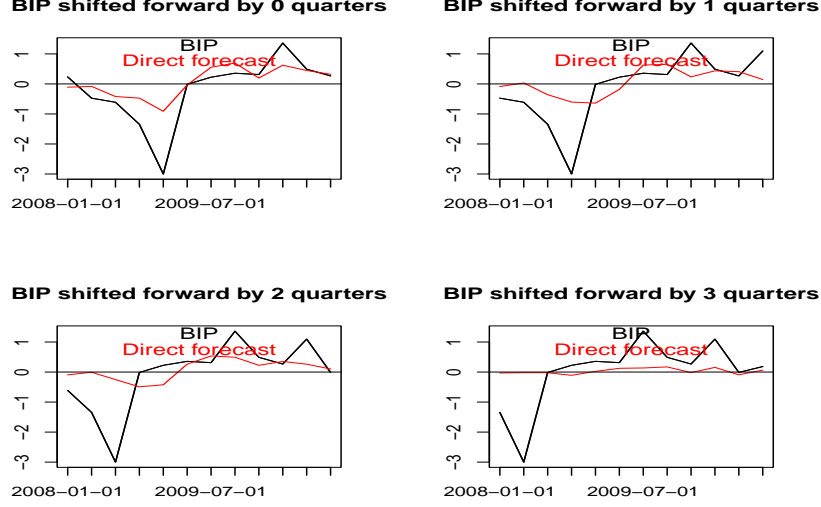
Figure 8: Direct forecast across the financial crisis.

The results indicate that as h increases, the peaks and dips of the direct forecasts become increasingly right-shifted (delayed) relative to the target. Additionally, the F-statistics precipitously decline from $F = 3.57$, for $h = 2$, to $F = 0.46$, for $h = 3$, see Table (1), suggesting that the predictor becomes statistically insignificant for larger forecast horizons exceeding two quarters (link to Heinisch and Scheufele).

3.2 Filter: HP(160)

As shown, the performance of direct forecasts sharply declines for larger forecast horizons. We conjecture that erratic short-term fluctuations -—unpredictable high-frequency noise -— overlay the data, thereby obscuring the effective 'signal' and making a direct regression more susceptible to overfitting. We therefore envisage to highlight the signal by applying a filter to dampen high-frequency noise. The so-called Hodrick-Prescott filter is a classic tool used in business cycle analysis: the filter is specified by a single smoothing parameter λ and the value $\lambda = 1600$ is specifically recommended for quarterly data. However, Phillips and Jin (2021) suggest that the HP(1600) filter removes relevant information due to excessive smoothing. In our context, this oversmoothing issue would be further exacerbated when considering forecast horizons shorter than a year -—an interval inconsistent with the mean duration of up to several years of business cycles, as highlighted by the HP(1600). Consequently, we here select a more adaptive HP(160) 'target' filter. While this choice may appear somewhat arbitrary, an analysis of the filter in the frequency domain confirms a more suitable profile for the corresponding amplitude function, assigning greater weight to yearly components -—relevant in our prediction framework-— than the classic quarterly HP filter. This approach also addresses and controls for undesirable high-frequency noise. See Fig. 9, which presents both two-sided and (classic) one-sided filters (top panels) along with the associated amplitude functions (bottom panels). We now posit the HP(160) filter as a means to achieve better forecasting performance at larger horizons, noting that a comprehensive technical analysis of the effect of λ on the resulting BIP predictor can be conducted using the M-SSA package.
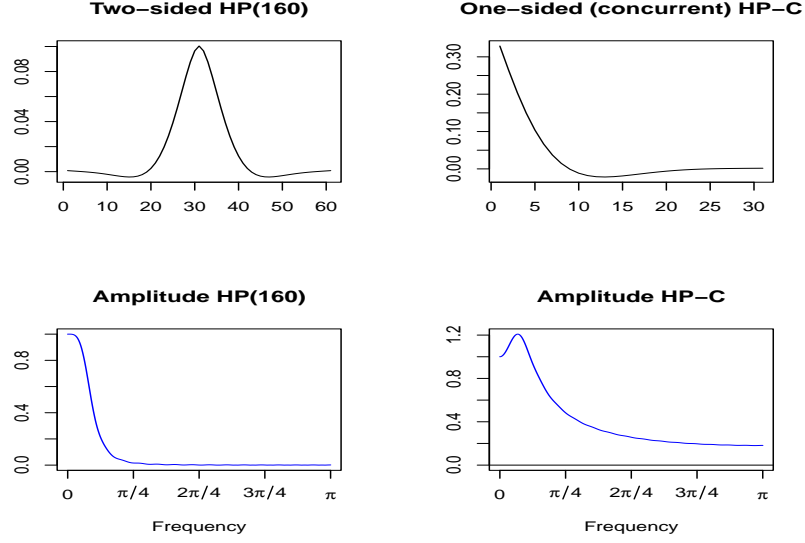
Figure 9: Two-sided HP-160) (top left) and one-sided (concurrent) HP-C filters (top right) with corresponding amplitude functions (bottom).

3.3 Direct HP Forecast

Extending the 'classic' direct forecast design, we here consider filtered indicators, based on the one-sided HP(160), denoted as HP-C: the filtered indicators are explanatory variables for the regressions on forward-shifted BIP[2]. As in the previous section, we rely on all indicators as well as the full sample estimate for illustration, see Figs.(10) (all observations with exclusion of the pandemic) and (11) (financial crisis). A comparison with the classic direct forecasts in Fig.(8) indicates that the new predictors are slightly less retarded ('faster').

---

[2]Katja and Simon: for each forecast horizon $h = 0, 1, 2, 3$ I'm using corresponding forecasts of the real-time filter output, assuming the data to be white noise (assuming an ARMA model does not lead to significantly different results). I think we might ignore these technical details in the paper.

BIP shifted forward by 0 quarters

BIP shifted forward by 1 quarters

BIP shifted forward by 2 quarters

BIP shifted forward by 3 quarters
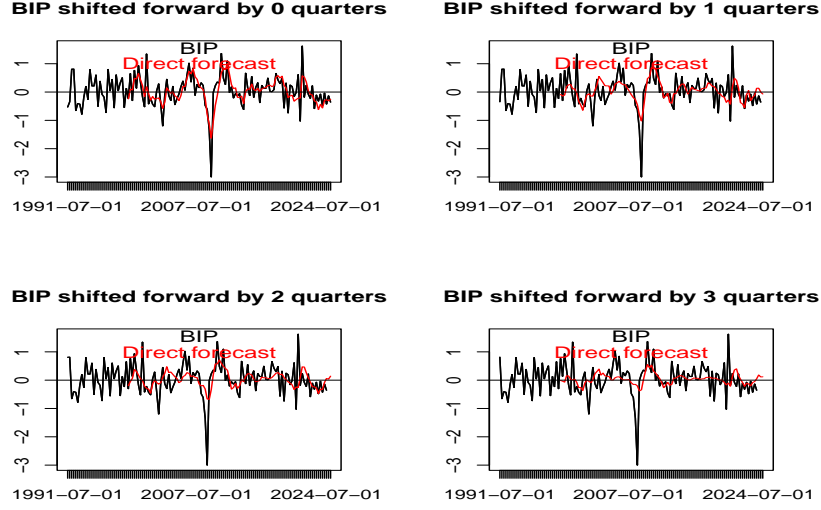
Figure 10: Direct HP forecasts: entire data set with exclusion of the pandemic.

BIP shifted forward by 0 quarters

BIP shifted forward by 1 quarters

BIP shifted forward by 2 quarters

BIP shifted forward by 3 quarters
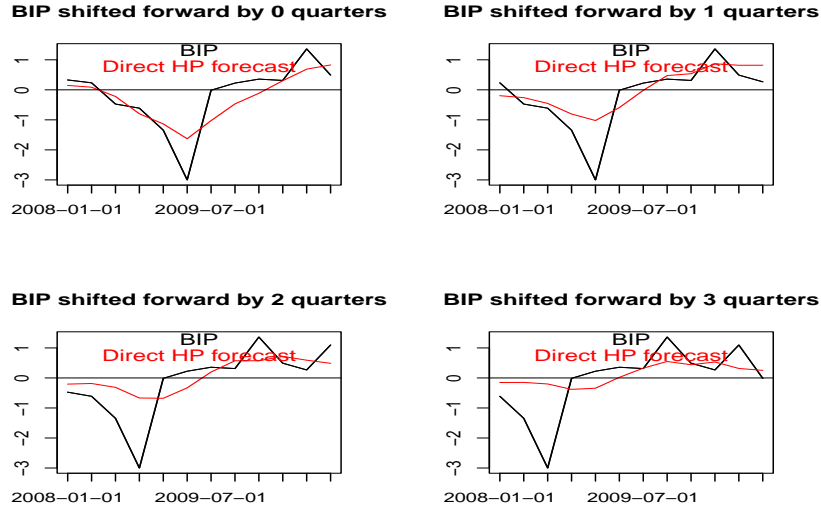
Figure 11: Direct HP forecasts over the curse of the financial crisis.

Moreover, the F-statistics are larger than for the direct forecasts, see Table (1), but the predictor remains statistically insignificant at forecast horizons exceeding two quarters (even though the evaluation is conducted in-sample and based on all available indicators). We now propose a more refined causal filter design aiming for statistical significance of the resulting predictor at longer forecast horizons, out-of-sample.

	h=0	h=1	h=2	h=3
Direct forecast	7.188	5.285	3.574	0.460
Direct HP forecast	21.886	8.415	4.810	1.834

Table 1: F-statistics of direct forecasts and direct HP forecasts for forecast horizons $h = 0, 1, 2, 3$: fully in-sample.

4 Multivariate Causal Filter: M-SSA

The application of the one-sided HP-C filter to the indicators has demonstrated improvements in forecast performance. However, the univariate nature of this filter limits its ability to leverage information from the cross-section, as supported by leading indicators. Additionally, the noise suppression capability of the one-sided filter is compromised, as illustrated by high-frequency leakage of the amplitude function in Fig. (9) and further elaborated upon by Wildi (2025). To address these limitations, we propose an extension of the Smooth Sign Accuracy (SSA) framework introduced by Wildi (2025).

4.1 Optimization criterion

Let $\mathbf{X}_t$ (of dimension $t \times n$) denote a set of n explanatory series $\mathbf{x}_{1t}, ..., \mathbf{x}_{nt}$, with observations $\mathbf{x}_{it} = (x_{i1}, ..., x_{it})'$. Let $\mathbf{z}_t = (z_1, ..., z_t)$ denote a target series, which typically lies outside the linear space spanned by $\mathbf{X}_t$ (and is unknown at time t). For simplicity, we assume stationarity of all time series involved. In this framework, $\mathbf{X}_t$ corresponds to a matrix of selected economic indicators with $n = 5$, and z_{it} is the output of a two-sided HP(160) filter applied to the i-th indicator, $i = 1, ..., 5$. Since z_{it} depends on future observations $x_{it+1}, x_{it+2}, ...$, the prediction task involves 'tracking' z_{it} using the estimate $y_t^i = \sum_{j=1}^n y_{jt}^i$, where $y_{jt}^i = \mathbf{b}_j^i{}' \mathbf{x}_{jt} = \sum_{k=0}^L b_{jk}^i x_{jk}$ are the outputs of a multivariate (causal or one-sided) filter $\mathbf{B}^i$, with columns $\mathbf{b}_j^i$ of fixed length L, $j = 1, ..., 5$, assigning weight to the last L observations of the j-th indicator $\mathbf{x}_{jt}$ (the fixed-length assumption is merely used for ease of exposition). For the sake of clarity, we now omit the upper-case index i for all variables, assuming $z_t = z_t^{i_0}$ for some fixed i_0. The task of 'tracking' a target can be formalized in different ways; here, we focus on the target correlation $\rho(z, y, h)$ between y_t and z_{t+h}, where $h \geq 0$ denotes the forecast horizon (backcasting with $h < 0$ is ignored in this context). To streamline the notation and avoid unnecessary complexity, we assume a fixed horizon, say $h = h_0$, so that we may drop the reference to h in our notation. In the univariate case ($n = 1$), Wildi (2025) proposes the Simple Sign Accuracy (SSA) as an optimization criterion for this task:

$$\left. \begin{array}{r} \rho(z, y) \to \max \\ \rho(y, 1) = \rho_1 \end{array} \right\}. \tag{1}$$

Objective function and constraint are expressed in terms of correlations, namely the target correlation $\rho(z, y)$ between target and predictor and the lag-one autocorrelation $\rho(y, 1)$ of the predictor. The parameter ρ_1 governs the smoothness of the predictor: higher values of ρ_1 generally promote smoother trajectories of y_t. Formally, assuming that the process x_t is centered (zero-mean), Wildi (2024) establishes a connection between $\rho(y, 1)$ and the expected duration between consecutive zero-crossings (sign changes) of y_t, the so-called holding time, denoted by $ht(y)$:

$$ht(y) = \frac{\pi}{\arccos(\rho(y, 1))}.$$

Since the non-linear transformation involved is strictly monotonic, the SSA criterion can be reformulated as the optimization problem:

$$\left. \begin{array}{r} \rho(z, y) \to \max \\ \frac{\arccos(\rho(y, 1))}{\pi} = 1/ht_1 \end{array} \right\}, \tag{2}$$

where the smoothness parameter $1/ht_1$ expresses the rate of zero-crossings of the predictor[3].

We now briefly discuss some implications of criterion (2). First, the objective function is indifferent to an affine transformation of the predictor. This ambiguity can be resolved by assuming an arbitrary scale and level for y_t (standardization). Alternatively, a mean-square error norm (MSE) may be substituted for the target correlation, as noted in Wildi (2025). In this case, the classic MSE predictor $y_{t,MSE}$ is obtained as a solution to the SSA criterion by insertion of $1/ht_1 := 1/ht_{MSE}$ in the constraint, where ht_{MSE} represents the holding time of $y_{t,MSE}$. Second, the concept can be extended to a multivariate framework, denoted as M-SSA, by generalizing the correlation functions, as detailed in Wildi (2025b). Lastly, sign changes in trend growth, represented by zero-crossings of the target z_t, are indicative of relevant changes in the trajectory of the economy, for example at transitions between expansions and recessions. Unfortunately, classic predictors often generate excessively many false 'noisy' crossings, due to high-frequency leakage as illustrated by the amplitude function in Fig. (9) (bottom right panel) and further elaborated upon by Wildi (2025). The SSA criterion helps control this phenomenon. More precisely, Wildi (2025) derives an equivalent dual formulation of criterion (2), which distinguishes the SSA solution as exhibiting the smallest rate of zero-crossings of any (linear) predictor with the same target correlation. We now rely on the M-SSA criterion to derive a 'smooth' predictor y_t of z_t.

4.2 M-MSE and M-SSA Nowcasts

For illustration, we consider the target z_t generated by the output of the two-sided HP(160) filter applied to BIP, which we denote by HP-BIP. We compare four nowcast methods: the univariate HP-C, the multivariate MSE predictor (denoted by M-MSE), and two M-SSA predictors based on different HT constraints. The first design enforces $ht_1 = 1.5ht_{MSE}$, aiming to produce approximately 33% fewer zero-crossings than the M-MSE predictor over the long term. The second design sets $ht_1 = ht_{HP-C}$, ensuring that its zero-crossing rate matches that of the univariate HP-C. These constraints are intended to systematically compare the effects of different levels of smoothness on prediction performance. The estimation of the underlying VAR(1) model employed for the M-MSE and M-SSA nowcasts is based on data observations up to January 2008. This approach ensures a lengthy out-of-sample period that encompasses significant events such as the financial crisis, the sovereign debt crisis, and the COVID-19 pandemic. Further details and background information are available in Wildi (2025b). All computations are performed utilizing the M-SSA package, as documented in Wildi (2025b). Figure 12 illustrates the coefficients of the multivariate filter designs, where increased smoothing achieved through the M-SSA method manifests as a distinct pattern in the filter weights, notably influencing the rate of decay across increasing lags. The resulting filtered series, presented in Figure 13, are standardized to enable direct comparisons. The two M-SSA predictors adhere to the specified constraints: one exhibiting approximately one-third fewer zero-crossings than the M-MSE, and the other matching the zero-crossing rate of the HP-C, confirming the effectiveness of the smoothness control imposed during the design. This is further corroborated by Table 2, which reports empirical holding times and target correlations. In this example, both the univariate design and the M-SSA method, when configured to replicate its holding time, demonstrate the highest level of smoothness, as indicated by the maximal duration between crossings. However, the HP-C also attains the lowest target correlation among the compared approaches. More generally, our example illustrates the prediction dilemma underlying the (M-)SSA criterion, highlighting the inherent trade-off between smoothness (zero-crossing rate) and predictive accuracy (target correlation).

---

[3]Formally, the exact relationship between the zero-crossing rate and the lag-one autocorrelation of the predictor assumes Gaussian time series, but Wildi (2024) demonstrates robustness to deviations from this assumption.
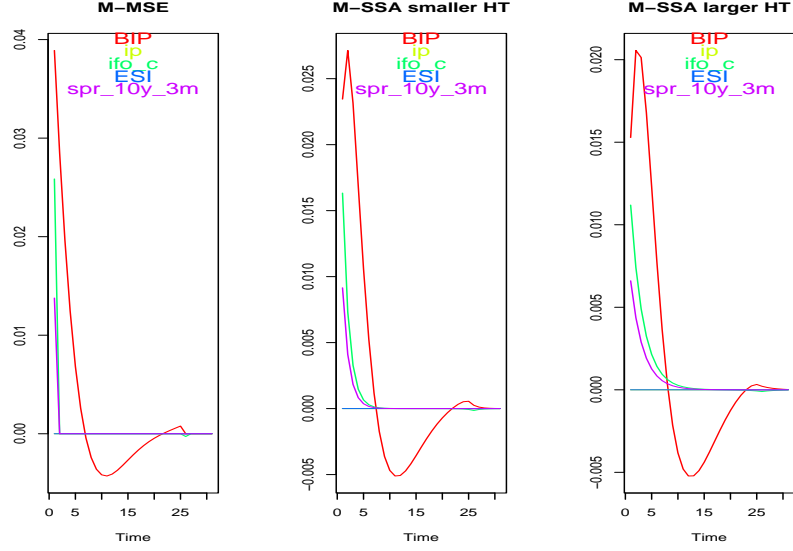
Figure 12: Multivariate M-MSE (left) and M-SSA (middle:smaller HT, right: larger HT) nowcast filters.
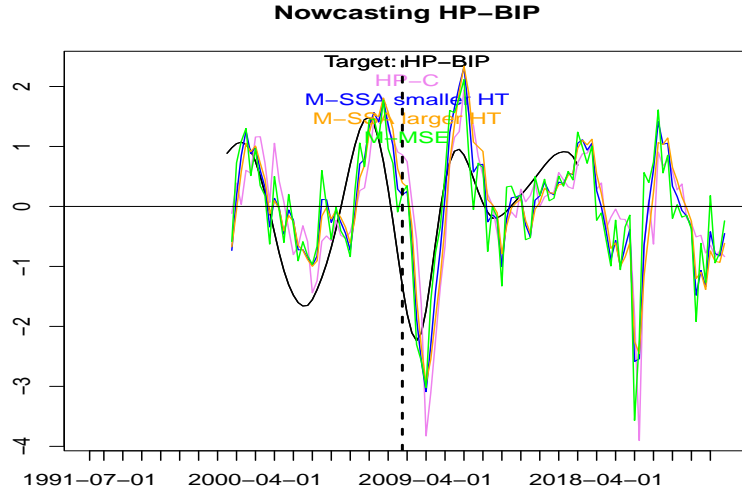
Figure 13: Nowcasting: two-sided HP(160) applied to BIP (target, black), univariate HP-C (violet), M-SSA smaller HT (blue), M-SSA larger HT (orange) and M-MSE (green). The dashed vertical line delimits in- and out-of-sample spans. The first L=31 observations are lost due to initialization and the two-sided filter does not extend to the sample end.

The results validate that the smoothing constraint incorporated into the multivariate extension of Criterion (1) effectively manages the zero-crossings of the predictor: sample estimates of the holding times (HTs) align with the expected values derived from Equation (2)[4]. An increase of approximately 50% in the HT relative to the M-MSE predictor has only a modest effect on the

―――――――――――――――

[4]Effective convergence of sample estimates to their theoretical expected values —assuming the true data-

	HP-C	M-SSA smaller HT	M-SSA larger HT	M-MSE
Target correlation	0.55	0.68	0.64	0.69
HT	8.67	6.50	7.43	3.71

Table 2: Target correlations and HTs of HP-C, M-SSA and M-MSE nowcasts.

target correlation, suggesting that this tradeoff could be beneficial in this application. Conversely, matching the HT of the HP-C predictor through M-SSA results in an increase in the target correlation, demonstrating the impact of zero-crossing control in the multivariate design on predictive performance. Going forward, we now omit the M-MSE, as it is a special case of the more general M-SSA framework.

4.3 M-SSA Forecasts

The previously described nowcast example can be systematically extended to generate forecasts of the target variable. This extension utilizes the same empirical framework, incorporating an assumed 50% increase in the HT over the M-MSE, and considers forward shifts of $h = 1, ..., 6$ quarters of HP-BIP (note that M-SSA does not target BIP explicitly). The influence of the forecast horizon on the M-SSA design is depicted in Fig. (14), which contrasts nowcast and one-year-ahead forecast: as h increases (right panel), the scaling factor diminishes (zero-shrinkage), attributable to increased forecast uncertainty, and there is a relative amplification of the influence of the relevant indicators, leading BIP in relative terms. Additionally, a phase shift associated with the filter applied to BIP is observed (red line, right panel), reflecting the cyclical characteristics inherent to the HP filter. While this phase effect might cause an effective sign change in the BIP filter output as h increases—something to be avoided in this context—the low-pass filters assigned to the additional 'leading' indicators (green and violet lines, right panel) continue to effectively track the low-frequency components of HP-BIP. The combination of the phase effect, applied to BIP, and level-tracking through these additional indicators enables more refined and effective tracking of the target compared to univariate forecasts, which rely solely on the phase-effect of the filter to look ahead of time.

M-SSA predictors are compared to the traditional univariate HP-C in Fig. (15) across the periods of the financial crisis (top panels) and the COVID-19 pandemic (bottom panels), for forecast horizons $h = 0, ..., 6$. The nowcast from the previous section is included for reference. All series are standardized to facilitate visual comparison. The primary distinction of the M-SSA approach is the progressive left-shift of the predictor as a function of h; this shift becomes more pronounced with increasing h and appears to be consistent across all levels, including the peaks and troughs of the series. Conversely, the positions of peaks and troughs in the HP-C series appear to remain largely unaffected by variations in h. The more pronounced and systematic left-shift observed in the M-SSA forecasts can be partly attributed to the increasing weight assigned to the additional indicators leading BIP, which dominate the BIP component at larger forecast horizons.

---

generating process is known— can be validated using the M-SSA package. This validation is typically performed through analyses of very long samples of simulated (multivariate) data, ensuring the consistency of the estimation procedures under idealized conditions.
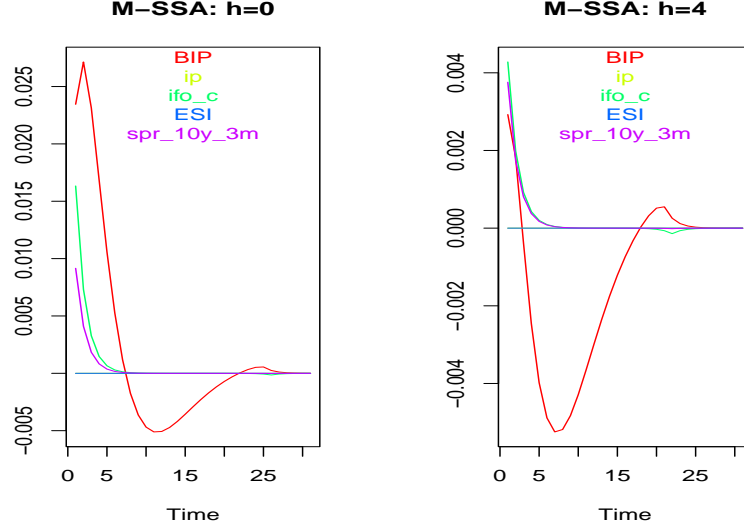
Figure 14: Multivariate M-SSA: $h = 0$ (nowcast, left) and $h = 4$ (one year forecast, right).
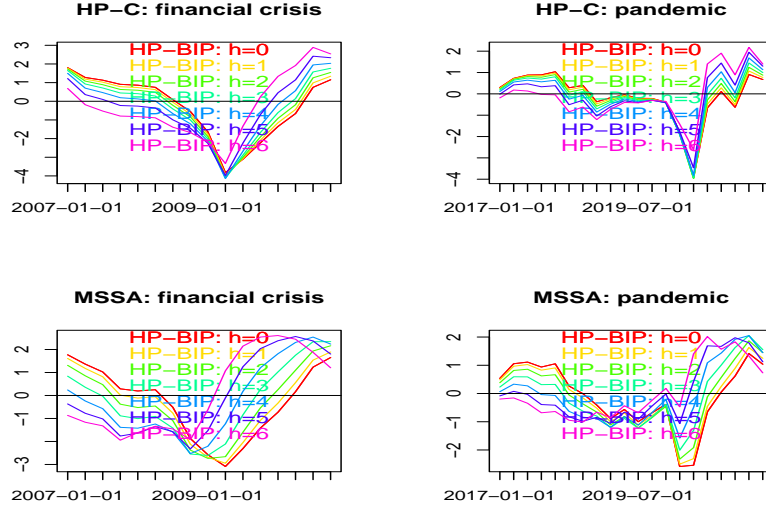
Figure 15: Now- and forecasts of HP-BIP for $h = 0, ..., 6$: HP-C (left) vs. M-SSA (right) across the financial crisis (top) and the pandemic (bottom).

5 M-SSA Component Predictor

The targets of the multivariate filters are the smoothed outputs obtained from the acausal two-sided HP(160) filter applied to the five indicators. However, our objective is to develop predictors that emphasize the unfiltered BIP. To achieve this, we can utilize the M-SSA outputs, referred to as M-SSA components.

5.1 Standardized Predictor: Equal-Weighting

Assuming that all M-SSA components contribute equally to BIP prediction, an initial step involves averaging the standardized components to form an equally-weighted composite measure. Subsequently, the predictor is derived by regressing this standardized aggregate on the (forward-shifted) BIP series. Fig. (16) presents the BIP series alongside the equally-weighted M-SSA predictor. All series are standardized to facilitate visual comparison and to highlight the dynamic shifts, particularly the left-shift characteristic of the predictors.

To enhance interpretability and assessment of the M-SSA predictor, we propose analyzing its individual components. For illustration, Fig. (17) shows the nowcast at $h = 0$. The solid blue line (the nowcast) approaches the zero line near the end of the sample, with a recent upward movement mainly supported by the leading spread component. In contrast, the ifo- and ESI-components remain near the zero line, while the ip- and BIP-components appear to be awaiting additional evidence and confirmation before signaling a definitive movement. This type of assessment can be useful for evaluating the relevance of recent changes in the forecasted time series dynamics.
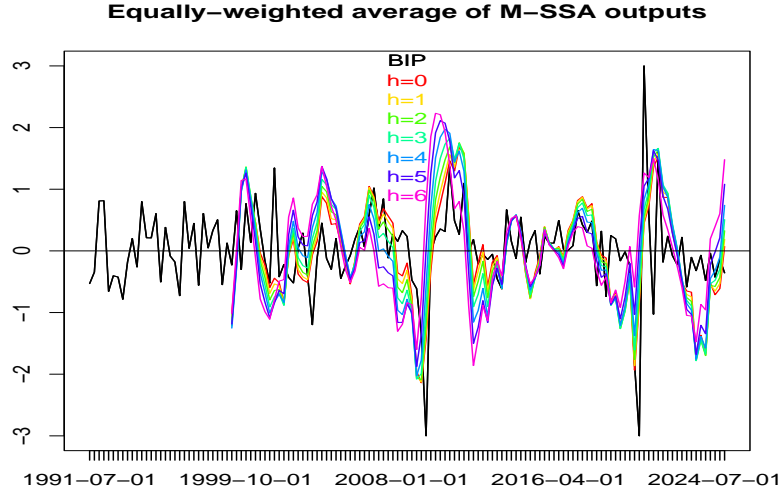

Figure 16: BIP and equally-weighted M-SSA predictor: all series standardized.
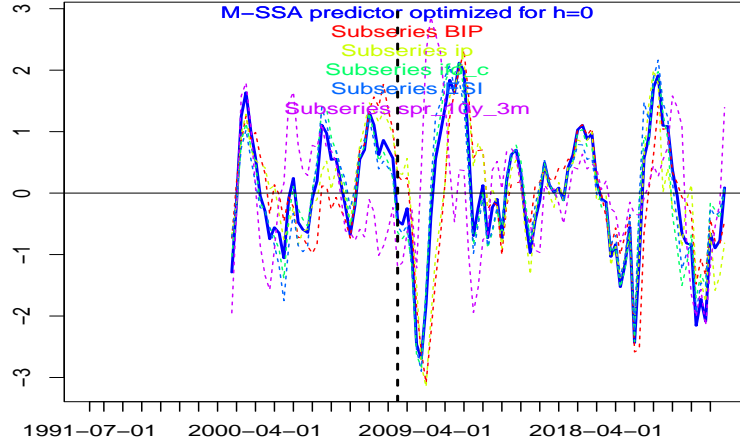
Figure 17: Equally-weighted M-SSA predictor and M-SSA components: all series standardized.

5.2 Tracking BIP: Optimal Weighting

We now utilize the M-SSA components as regressors on forward-shifted BIP, extending the previous (standardized) equally-weighted M-SSA predictor to incorporate optimal weighting of the components. While we keep the M-SSA fixed, as based on data up to January 2008, we implement an expanding window starting from January 2007 for deriving the component weights, which are up-dated on a quarterly basis (this contrasts with Section (3) which was based on the full sample information).

There are various combinations of M-SSA components for tracking BIP. For illustration, we here select the single BIP component resulting from the M-SSA filter tracking HP-BIP. Table (3) reports HAC-adjusted p-values from regressions of the out-of-sample predictor on HP-BIP, indicating a strong link between the predictor and the target, out-of-sample. Our choice—focusing

	h=0	h=1	h=2	h=3	h=4	h=5	h=6
Shift=0	0.000	0.000	0.001	0.002	0.005	0.020	0.112
Shift=1	0.000	0.000	0.000	0.001	0.002	0.005	0.019
Shift=2	0.000	0.000	0.000	0.001	0.001	0.003	0.006
Shift=3	0.018	0.007	0.002	0.000	0.002	0.003	0.004
Shift=4	0.180	0.100	0.040	0.010	0.002	0.005	0.005
Shift=5	0.579	0.432	0.261	0.108	0.027	0.008	0.009

Table 3: HAC adjusted p-values of regressions of BIP (M-SSA) component optimized for forecast horizons $h = 0, ..., 6$ (the columns) on HP-BIP shifted forward by shift=0,...,5 (the rows). Out-of-sample span starting in Jan-2007, without pandemic.

on the single M-SSA BIP component—emphasizes simplicity and interpretability, as future BIP and HP-BIP are connected through their shared low-frequency component. Additionally, the M-SSA BIP component is the most important predictor in the regression of the M-SSA outputs on BIP. Finally, revisions due to quarterly updates of the regression equations are minimized by this predictor, and the estimates are more stable and robust over time[5] (see Section (6)). Note that

---

[5]Other combinations can be experimented with using the M-SSA package. Regression weights of more complex

information from the other indicators is incorporated into the M-SSA BIP component through the multivariate filter design.

This setup allows us to evaluate the out-of-sample performance of various predictor approaches, including: (i) the simple mean of BIP, (ii) the direct forecast method described in Section (3.1), (iii) the direct HP forecasts from Section (3.3), based on the univariate HP-C, and (iv) the new M-SSA BIP component predictor.

5.3 Out-of-Sample Forecast Performances

Tables (4) and (5) present HAC-adjusted p-values and rRMSEs for the BIP component predictor. The p-values are obtained from a regression of the out-of-sample predictor on forward-shifted BIP (in contrast to Table (3), which emphasized HP-BIP); hence, they do not account for potential bias or mis-scaling of the predictor. In contrast, the rRMSEs, evaluated against the mean benchmark, do incorporate eventual bias and mis-scaling effects. Additional results involving other predictor benchmarks are provided in the appendix, based on data sets with and without the pandemic. The results can be summarized as follows: targeting future HP-BIP (see Table (3)) is less challenging than predicting BIP (see Table (4)), due to smoothness (autocorrelation) of the target when compared to BIP. The pandemic period generally obscures the relationships between predictors and BIP. When excluding the pandemic, the direct forecasts outperform the mean forecast up to two quarters ahead. The M-SSA component predictor, optimized for longer forecast horizons, outperforms the mean benchmark up to one year ahead. Additionally, the BIP component predictor also surpasses the direct forecasts for larger forecast horizons ($h > 2$ quarters). Statistical significance of the BIP component predictor, optimized for larger forecast horizons, can be established for at least up to one year ahead. Predictors optimized for $h \geq 4$ generally outperform the other designs, irrespective of the forward-shift of BIP.

	h=0	h=1	h=2	h=3	h=4	h=5	h=6
Shift=0	0.084	0.047	0.017	0.005	0.002	0.001	0.038
Shift=1	0.230	0.160	0.094	0.032	0.005	0.001	0.004
Shift=2	0.801	0.666	0.414	0.173	0.026	0.005	0.006
Shift=3	0.876	0.961	0.917	0.683	0.248	0.068	0.039
Shift=4	0.370	0.819	0.990	0.953	0.533	0.117	0.030
Shift=5	0.353	0.802	0.983	0.943	0.571	0.239	0.043

Table 4: HAC adjusted p-values of regressions of M-SSA component predictors optimized for forecast horizons $h = 0, ..., 6$ (the columns) on BIP shifted forward by shift=0,...,5 (the rows). Out-of-sample span starting in Jan-2007, without pandemic.

	h=0	h=1	h=2	h=3	h=4	h=5	h=6
Shift=0	0.978	0.942	0.893	0.855	0.860	0.906	0.962
Shift=1	1.082	1.060	1.005	0.926	0.877	0.880	0.914
Shift=2	1.083	1.090	1.077	1.019	0.952	0.918	0.919
Shift=3	1.034	1.059	1.081	1.063	1.010	0.970	0.954
Shift=4	0.995	1.029	1.069	1.077	1.035	0.986	0.953
Shift=5	0.993	1.030	1.075	1.093	1.062	1.011	0.967

Table 5: rRMSEs of M-SSA components predictor benchmarked against the expanding mean of BIP. Out-of-sample span starting in Jan-2007, without pandemic.

---

designs, involving multiple components, tend to be more difficult to interpret due to the occurrence of negative weights and potential sign changes of the regressors over time, which may indicate overfitting or non-stationarity.

6 Revisions

Revisions refer to changes in the historical values of a time series resulting from updates with new information. Revisions of the M-SSA component predictor can arise from data updates, which we do not analyze further here[6], or from updates to predictor parameters. The latter can be further separated into changes in VAR parameters and regression weights.

6.1 Revisions: Regression Equation Only

For illustration, we here focus on a forecast horizon $h = 4$ for the BIP component predictor and a forward-shift $shift = 4$ for BIP, noting that similar results would be obtained with other combinations of h and $shift$. Fig.(18) compares the final and real-time predictors: as the sample size increases, the real-time predictor converges steadily to the final predictor and the rate of convergence is partially determined by the simplicity of our design, which avoids incorporating additional M-SSA components. As a confirmation, Fig.(19) displays the evolution of the intercept and regression weights over time: with increasing sample size, these estimates seem to converge to fixed points, indicating both the stationarity of the process and the consistency of the estimates (note, however, the slightly elevated values of the regression weight assigned to the M-SSA component during the financial crisis and the pandemic, suggesting a stronger link between the target and the predictor). In contrast, more complex designs based on multiple M-SSA components can exhibit substantial fluctuations in the regression parameters, sometimes changing signs. This suggests instability and complicates interpretation.
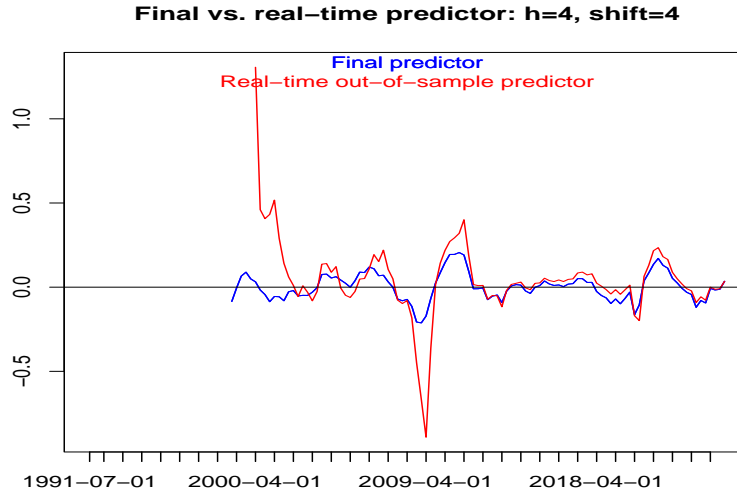
Figure 18: Revisions of the M-SSA BIP component predictor are shown, with the final predictor in blue and the real-time design in red. These revisions result from quarterly updates to the regression equations. The M-SSA filter itself remains fixed, based on data up to January 2008.

---

[6]Except for BIP, the other indicators are not or only slightly revised. Moreover, the smoothing effect of filters mitigates the effect of revisions when compared to direct forecasts.

Intercept and regression weight over time: h=4, shift=4
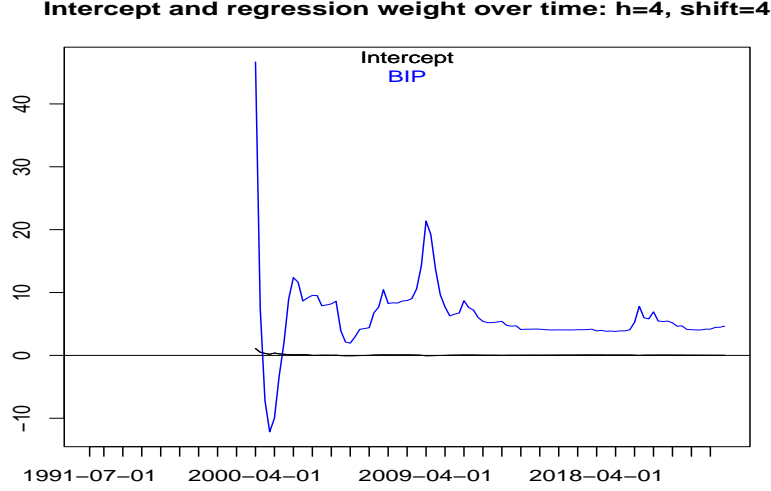
Figure 19: Revisions of intercept and regression weight.

6.2 Revisions: M-SSA Only

The second source of revisions in the M-SSA component predictor arises from updates to the VAR model within the M-SSA filter. We compare the original estimates, based on data up to January 2008, with the final estimates obtained using $h = 4$ and $shift = 4$ (similar findings apply to other values of forecast horizon and forward-shift). For consistency, we excluded the entire pandemic episode from the data. Fig.(20) compares the MA-inversions (impulse responses) of the BIP equation derived from the 'old' and the updated VAR models: unlike the former, the latter incorporates ESI as an additional explanatory variable for BIP. Fig.(21) illustrates the resulting effect on the M-SSA filter targeting HP-BIP at forecast horizon $h = 4$. The updated filter (right panel) assigns more weight to the additional 'leading' indicators relative to BIP. Finally, Fig.(22) compares the M-SSA BIP predictors. To isolate the effect of the regression revision, the figure displays standardized series. The update to the VAR model influences the left-shift of the predictor (blue line), which appears slightly 'faster' than the original predictor (red line). This suggests that the out-of-sample performance of the M-SSA component predictor may be better than reported in Section (5.3), which is based on the fixed and increasingly outdated version of M-SSA.
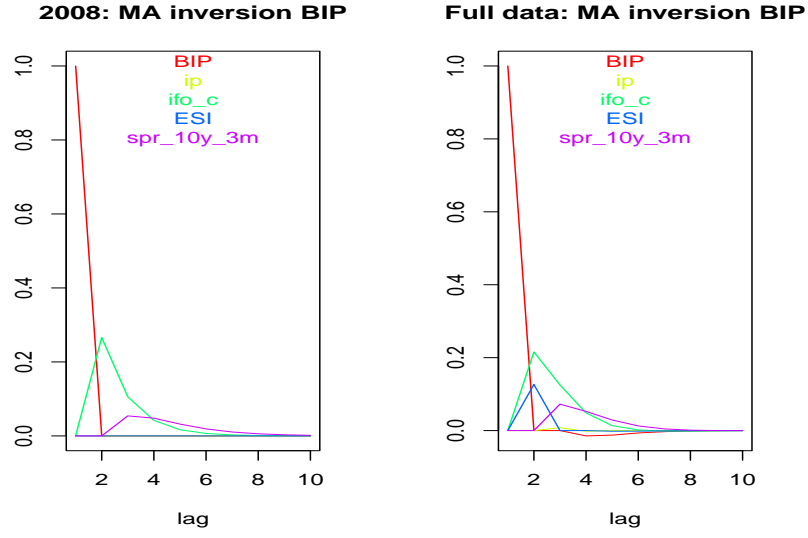
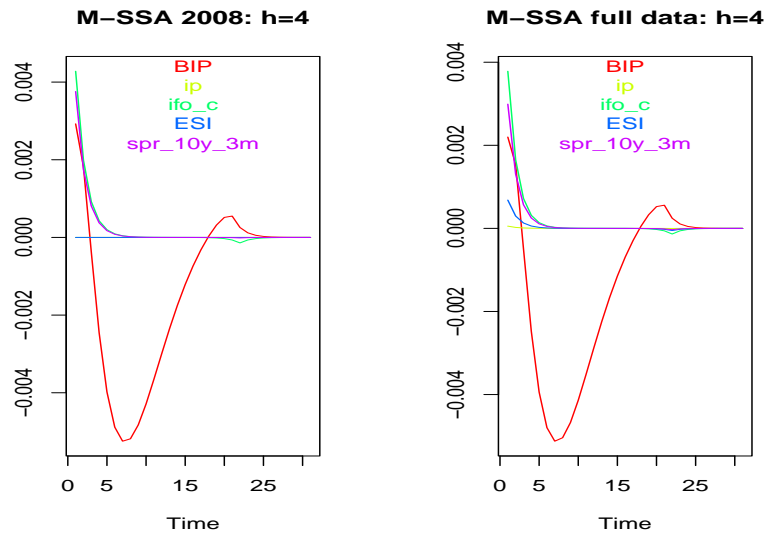Figure 20: MA-inversion (impulse response) of VAR: data up to Jan-2008 (left) vs. entire data set (right).

Figure 21: M-SSA filter tracking HP-BIP at forecast horizon $h = 4$: data up to Jan-2008 (left) vs. entire data set (right).

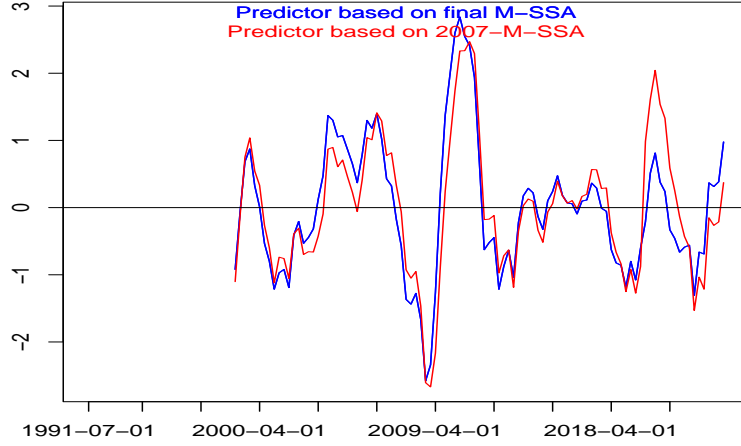**BIP component predictors: final and 2007−MSSA (h=4, shift=4**

Figure 22: Revisions resulting from updates to the VAR model in M-SSA. To isolate the effect of the regression revision, all series are standardized. The up-dated M-SSA (blue) is left-shifted at the zero-crossings and appears slightly faster. For consistency, the entire pandemic episode has been removed.

7 Summary and Conclusion

Classic direct forecasts of BIP can outperform simple benchmarks, such as the mean, up to two quarters ahead. However, this limited forecast horizon is often insufficient for certain applications. A key challenge with direct forecasts is that the relevant indicators tend to be noisy, which can mask the true signal and lead to overfitting. In particular, the predictor struggles to timely track dips (slowdowns, recessions) or peaks (recoveries, expansions). To address this issue, we apply a HP(160)-filter to smooth the data, with the smoothing parameter $\lambda = 160$ reflecting a more adaptive design than the classic quarterly HP, in line with an intended forecast horizon of up to one year ahead. The resulting predictor tends to outperform the classic direct forecasts in terms of statistical significance, mainly due to a slight left-shift noticeable at sharp recession dips. However, despite the filtering, the predictor remains somewhat noisy, potentially producing excessive noisy zero-crossings at the transitions between recessions and expansions. This issue is partly due to noise leakage inherent in the one-sided HP filter.

To address these problems, we propose a multivariate extension of SSA based on Wildi (2024). Unlike the univariate HP filter, the M-SSA can leverage cross-sectional information from indicators leading BIP in real time while controlling for the rate of zero-crossings of the predictor. Consequently, the multivariate filter outputs become increasingly left-shifted as the forecast horizon lengthens, allowing dips and peaks of the target series to be tracked more systematically, while reducing the occurrence of noisy zero-crossings. However, since M-SSA does not explicitly target BIP, an additional step is necessary to derive the final BIP predictor. We propose two approaches: a simple equally-weighted aggregate, assuming all M-SSA components are equally important for predicting BIP, and an optimally weighted predictor based on a regression of the M-SSA components on future BIP.

For illustration, we consider a simple approach based on regressing the single M-SSA BIP output on future BIP, thereby ignoring the other filter outputs. This predictor is intuitively ap-

20

pealing because the future HP-BIP—i.e., the target of M-SSA—is the low-frequency component of the future BIP target. Consequently, a strong link between M-SSA and future HP-BIP also indicates a connection with BIP, even if the statistical significance is obscured by the noise inherent in BIP. Out-of-sample performance suggests that this predictor is statistically significant at horizons up to one year. Moreover, designs optimized for larger forecast horizons outperform the mean benchmark at all considered forecast horizons, and the predictor exceeds the performance of direct forecasts—based on unfiltered or HP filtered indicators—at horizons longer than two quarters. An analysis of revision errors arising from quarterly updates of the proposed M-SSA BIP component predictor indicates that the regression parameters, the VAR model, and the resulting M-SSA filters stabilize after an initial burn-in period. This stability enhances the explainability and interpretability of the predictor.

In conclusion, the new predictor design integrates the traditional direct forecast approach with a novel multivariate filter to target BIP up to one year ahead. This multivariate approach leverages a set of economic indicators leading BIP in real time while controlling the smoothness of the predictor through the zero-crossing rate.

8   Appendix

8.1   Performances: Without Pandemic

	h=0	h=1	h=2	h=3	h=4	h=5	h=6
Shift=0	0.084	0.047	0.017	0.005	0.002	0.001	0.038
Shift=1	0.230	0.160	0.094	0.032	0.005	0.001	0.004
Shift=2	0.801	0.666	0.414	0.173	0.026	0.005	0.006
Shift=3	0.876	0.961	0.917	0.683	0.248	0.068	0.039
Shift=4	0.370	0.819	0.990	0.953	0.533	0.117	0.030
Shift=5	0.353	0.802	0.983	0.943	0.571	0.239	0.043

Table 6: HAC adjusted p-values of regressions of M-SSA component predictors optimized for forecast horizons $h = 0, ..., 6$ (the columns) on BIP shifted forward by shift=0,...,5 (the rows). Out-of-sample span starting in Jan-2007, without pandemic.

	h=0	h=1	h=2	h=3	h=4	h=5	h=6
Shift=0	0.978	0.942	0.893	0.855	0.860	0.906	0.962
Shift=1	1.082	1.060	1.005	0.926	0.877	0.880	0.914
Shift=2	1.083	1.090	1.077	1.019	0.952	0.918	0.919
Shift=3	1.034	1.059	1.081	1.063	1.010	0.970	0.954
Shift=4	0.995	1.029	1.069	1.077	1.035	0.986	0.953
Shift=5	0.993	1.030	1.075	1.093	1.062	1.011	0.967

Table 7: rRMSEs of M-SSA components predictor benchmarked against the expanding mean of BIP. Out-of-sample span starting in Jan-2007, without pandemic.

	h=0	h=1	h=2	h=3	h=4	h=5	h=6
Shift=0	1.144	1.102	1.045	0.999	1.006	1.059	1.125
Shift=1	1.238	1.213	1.151	1.060	1.004	1.007	1.047
Shift=2	1.178	1.186	1.171	1.108	1.035	0.999	0.999
Shift=3	1.011	1.035	1.057	1.039	0.988	0.948	0.933
Shift=4	1.010	1.045	1.086	1.094	1.051	1.002	0.968
Shift=5	0.982	1.019	1.064	1.081	1.051	1.000	0.957

Table 8: rRMSEs of M-SSA components predictor benchmarked against the direct forecasts. Out-of-sample span starting in Jan-2007, without pandemic.

	h=0	h=1	h=2	h=3	h=4	h=5	h=6
Shift=0	0.855	0.855	0.855	0.855	0.855	0.855	0.855
Shift=1	0.874	0.874	0.874	0.874	0.874	0.874	0.874
Shift=2	0.919	0.919	0.919	0.919	0.919	0.919	0.919
Shift=3	1.023	1.023	1.023	1.023	1.023	1.023	1.023
Shift=4	0.985	0.985	0.985	0.985	0.985	0.985	0.985
Shift=5	1.010	1.010	1.010	1.010	1.010	1.010	1.010

Table 9: rRMSEs direct forecasts benchmarked against the expanding mean. Out-of-sample span starting in Jan-2007, without pandemic.

8.2 Performances: Including Singular Pandemic Data

	h=0	h=1	h=2	h=3	h=4	h=5	h=6
Shift=0	0.127	0.064	0.019	0.003	0.001	0.002	0.012
Shift=1	0.439	0.314	0.194	0.093	0.033	0.017	0.036
Shift=2	0.718	0.565	0.326	0.098	0.020	0.008	0.010
Shift=3	0.946	0.975	0.925	0.657	0.222	0.059	0.028
Shift=4	0.327	0.699	0.964	0.942	0.619	0.237	0.102
Shift=5	0.383	0.755	0.946	0.910	0.581	0.241	0.055

Table 10: HAC adjusted p-values of regressions of M-SSA component predictors optimized for forecast horizons $h = 0, ..., 6$ (the columns) on BIP shifted forward by shift=0,...,5 (the rows). Out-of-sample span starting in Jan-2007, including the pandemic.

	h=0	h=1	h=2	h=3	h=4	h=5	h=6
Shift=0	1.008	0.990	0.964	0.939	0.930	0.942	0.967
Shift=1	1.064	1.057	1.036	1.001	0.976	0.968	0.973
Shift=2	1.033	1.034	1.026	0.999	0.969	0.955	0.957
Shift=3	1.025	1.034	1.040	1.028	1.001	0.979	0.967
Shift=4	0.995	1.011	1.030	1.037	1.022	1.003	0.990
Shift=5	1.001	1.018	1.039	1.048	1.034	1.009	0.986

Table 11: rRMSEs of M-SSA components predictor benchmarked against the expanding mean of BIP. Out-of-sample span starting in Jan-2007, including the pandemic.

	h=0	h=1	h=2	h=3	h=4	h=5	h=6
Shift=0	1.210	1.188	1.157	1.127	1.116	1.130	1.161
Shift=1	0.982	0.977	0.957	0.925	0.902	0.895	0.899
Shift=2	1.053	1.054	1.046	1.018	0.987	0.973	0.975
Shift=3	1.046	1.056	1.062	1.050	1.022	0.999	0.988
Shift=4	0.969	0.984	1.003	1.010	0.996	0.977	0.964
Shift=5	0.982	0.998	1.019	1.027	1.014	0.990	0.967

Table 12: rRMSEs of M-SSA components predictor benchmarked against the direct forecasts. Out-of-sample span starting in Jan-2007, including the pandemic.

	h=0	h=1	h=2	h=3	h=4	h=5	h=6
Shift=0	0.833	0.833	0.833	0.833	0.833	0.833	0.833
Shift=1	1.083	1.083	1.083	1.083	1.083	1.083	1.083
Shift=2	0.981	0.981	0.981	0.981	0.981	0.981	0.981
Shift=3	0.979	0.979	0.979	0.979	0.979	0.979	0.979
Shift=4	1.027	1.027	1.027	1.027	1.027	1.027	1.027
Shift=5	1.020	1.020	1.020	1.020	1.020	1.020	1.020

Table 13: rRMSEs direct forecasts benchmarked against the expanding mean. Out-of-sample span starting in Jan-2007, including the pandemic.